Comparison of Wind Tunnel Measurements with NBCC 2010 Wind-Induced Torsion Provisions for Low- and Medium-Rise Buildings

Mohamed Elsharawy
Ph.D. Candidate, Dept. of Building, Civil and Environmental Engineering, Centre for Building Studies, Concordia University, Montréal, Québec (H3G 1M8), Canada
(Corresponding author, m_els@encs.concordia.ca)

Khaled Galal
Associate Professor, Dept. of Building, Civil and Environmental Engineering, Concordia University, Montréal, Québec (H3G 1M8), Canada

Ted Stathopoulos
Professor, Dept. of Building, Civil and Environmental Engineering, Centre for Building Studies, Concordia University, Montréal, Québec (H3G 1M8), Canada

Word count: 8629

Abstract

The aim of this study is to assess wind-induced torsional loads on low- and medium-rise buildings determined in accordance with the National Building Code of Canada (NBCC 2010). Two building models with the same horizontal dimensions but different gabled-roof angles (0^o and 45^o) were tested at different full-scale equivalent eave heights (6, 12, 20, 30, 40, 50 and 60 m) in open terrain exposure for several wind directions (every 15^o). Wind-induced measured pressures were numerically integrated over all building surfaces and results were obtained for along-wind force, across-wind force, and torsional moment. Torsion load case (i.e. maximum torsion and corresponding shear) and shear load case (i.e. maximum shear and corresponding torsion) were evaluated to reflect the maximum actual wind load effects in the two horizontal directions (i.e. transverse and longitudinal). The evaluated torsion and shear load cases were also compared with the current torsion- and shear-related provisions in the NBCC 2010. The results demonstrated significant discrepancies between NBCC 2010 and the wind tunnel measurements regarding the evaluation of torsional wind loads on low- and medium-rise buildings. Finally, shear and torsion load cases were suggested for evaluating wind loads in the design of low- and medium-rise rectangular buildings.

Key words: Wind loads, Torsion, Shear, Wind provisions, Low-rise buildings, Medium-rise buildings

1 Introduction

Proper building design against wind loads depends primarily on the adequacy of the provisions of codes of practice and wind load standards. During the past decades, much has been learned about along- and across-wind forces on buildings. However, studies on wind-induced torsional loads on buildings are very limited. The recent trends towards construction of more complex building shapes and structural systems can result in an increase of the unbalanced wind loads yielding an increase of torsional moments. Thus, re-visiting the wind load provisions is of an utmost concern to ensure their adequacy in evaluating torsion on low- and medium-rise buildings and consequently, achieve safe, yet economic building design. It is noteworthy that most of the wind loading provisions on torsion have been developed from the research work largely directed towards very tall and flexible buildings (Melbourne, 1975, Vickery and Basu, 1984, Boggs et al. 2000) for which resonant responses are significant. However, the dynamic response of most medium-rise buildings is dominated by quasi-steady gust loading with little resonant effect. Moreover, the lack of knowledge regarding wind-induced torsion is reflected in having different approaches in evaluating torsion in the international wind loading codes and standards.

Tamura et al. (2008) and Keast et al. (2012) studied wind load combinations that included torsion for medium-rise buildings. The former study showed the importance of the wind load combinations including torsion on the peak normal stress generated in the building columns. Based on testing of a limited number of building models, the latter study concluded that for rectangular buildings the peak overall torsion occurs simultaneously with 30-40% of the peak overall drag force. Further experimentations with different building configurations are still required to confirm and generalize these results.

Very few studies have examined wind-induced torsional loads on low-rise buildings. Isyumov and Case (2000) measured wind-induced torsion on three low-rise buildings with different aspect ratios (length/width = 1, 2, 3) in open terrain exposure modeled in the wind tunnel. The study suggested that applying partial wind loads, similar to those implemented for the design of medium-rise buildings, would improve the design of low-rise buildings until more pertinent data become available. Tamura et al. (2001) examined the correlation of torsion with along-wind and across-wind forces for rectangular low-rise buildings tested in simulated open and urban terrain exposures. Low-rise buildings of different roof slopes were also tested by Elsharawy et al. (2012). Good agreement was found when the results were compared with Isyumov and Case (2000) study for similar tested cases (i.e. low-rise buildings with gable-roof slope 4:12). It was also concluded that the peak torsions evaluated using current wind provisions of standards and codes of practise are different from those measured in the wind tunnel.

This paper reports on the analysis and code comparison of results of additional measurements carried out in a boundary layer wind tunnel to investigate shear forces occurring simultaneously with maximum torsion, as well as maximum shears and corresponding torsions on buildings of different roof slopes and heights. Results of the study are important for the appropriate evaluation of wind-induced torsional loads on buildings.

2 Wind loads including torsion in NBCC 2010

The National Building Code of Canada was the first to adopt in its provisions the effect of wind-induced torsional loads on buildings. Since the early 70's and until 2005, the NBCC has included unbalanced wind loads to generate wind-induced torsion on medium-rise buildings. In fact, it was suggested to remove 25% of the full wind load from any portion on building surfaces in

order to maximize torsion according to the most critical design scenario states. This allowance for torsion is equivalent to applying the full design wind load at an eccentricity, which was 3 or 4 percent of the building width. In the NBCC 2005 edition, the 25% removal of the full wind load has been modified into a complete removal of the full wind loads from those areas that would lead to maximize torsion. Accordingly, limiting the load on half of windward and leeward building faces will generate torsion, equivalent to applying the full design wind load at an eccentricity equal to 12.5 percent of the horizontal dimension perpendicular to the wind direction.

In NBCC (2010), the static method specifies wind loads on low-rise buildings (defined as having mean roof height, $h < 10$ m, or $h < 20$ m and $h <$ smallest horizontal building dimension, B). One load case is described in the static approach to evaluate maximum shear, as well as maximum torsion. The simplified method is suggested for medium-rise buildings, defined as having $h < 60$ m, $h/B < 4$, and lowest natural frequency, $f_n > 1$ Hz. It is important to mention that most of the torsion provisions in the simplified method were revealed from testing very tall and flexible buildings (Isyumov (1982), ASCE (1999)). The method identifies four load cases: in Cases A and C, symmetric uniform loads are considered, in order to estimate the maximum base shears and overturning moments; and, in Cases B and D partial wind loads are recommended to create equivalent torsional building loads. Nevertheless, the choice of partial loads could be difficult for design engineers following the code statements quoted below:

> *"In case B, the full wind pressure should be applied only to parts of the wall faces so that the wind-induced torsion is maximized" (note (2) to figure I-16); and*

> *"To account for potentially more severe effects induced by diagonal wind, and also for the tendency of structures to sway in the cross-wind direction, taller structures should be designed to resist 75% of the maximum wind pressures for each of the principal directions applied*

simultaneously as shown in figure I-16, Case C. In addition, the influence of removing 50% of the case C loads from parts of the face areas that maximizes torsion, as shown in figure I-16, case D, should be investigated" (Commentary I, paragraph 37)."

As can be noted, it might not be easy to determine the parts of the wall faces on which the reduced wind loads should be applied in order to account for the appropriate torsion and shear combinations needed for a proper design of the building.

3 Wind tunnel tests

The experiments were carried out in the boundary layer wind tunnel of Concordia University. The working section of the tunnel is approximately 12.2 m long x 1.80 m wide. Its height is adjustable and ranges between 1.4 and 1.8 m to maintain negligible pressure gradient for different simulated exposures along the test section. A turntable of 1.2 m diameter is located on the test section of the tunnel and allows testing of models for any wind direction. An automated traversing gear system provides the capability of probe placement to measure wind characteristics at any spatial location around a building model inside the test section. A minimum geometric scale of 1:400 has been recommended for the simulation of the most important variables of the atmospheric boundary layer under strong wind conditions.

3.1 Building models

Figure 1 shows the two building models, with 0^o and 45^o gabled-roof angles, instrumented with 146 and 192 pressure taps on their surfaces, respectively. The flat roof does not have any pressure taps since uplift forces do not contribute to torsion or horizontal shear forces. The models were tested for seven different heights. By sliding them in a fitted slot in the turntable, buildings with eave heights of 6, 12, 20, 30, 40, 50 and 60 m were represented. Model and

equivalent full scale dimensions of the tested buildings are given in Table 1. In this study, all tested buildings were assumed to be structurally rigid and follow the limitations stated in NBCC 2010. The models were enclosed, since internal pressures were not considered in this study.

3.2 Terrain simulations

An open-country exposure was simulated in the wind tunnel. The flow approach profiles of mean wind velocity and turbulence intensity were measured using a 4-hole Cobra probe (TFI) for the simulated terrain exposure (see Figure 2). The wind velocity at free stream was 13.6 m/s. The power law index α of the mean wind velocity profile was set at $\alpha = 0.15$. Although the majority of medium height buildings are situated in suburban terrain, an open exposure was considered as higher overall wind loads are expected, as discussed in Elsharawy et al. (2012). However, it is also recognized that rougher terrain exposure, in some cases, may result in greater unbalancing of wind loads and torsion. Additionally, since building models are symmetric in both directions and located in open terrain exposure, the tested wind directions were limited to the interval of 0^o to 90^o. The pressure measurements on the models were conducted using a system of miniature pressure scanners from Scanivalve (ZOC33/64Px) and the digital service module DSM 3400. A standard tubing system was used in these measurements, in order to minimize the Gain and Phase shifts of pressure signals due to Helmholtz's resonance effects. Corrections were made by using traditional restrictors properly calibrated. The pressure measurement tubes have an outer and inner diameter of 2.18 and 1.37 mm respectively, their length is 55 cm and restrictors are installed at 30 cm from the location of the pressure tap. All measurements were synchronized with a sampling rate of 300 Hz on each channel for a period of 27 sec (i.e. about one hour in full scale). It is known that the mean wind speed is relatively steady over short periods of time (say

10 minutes to an hour), i.e. it is stationary, as reported by Van der Hoven (1957). This period is also suitable to capture all gust loads, which may be critical for structural design.

4 Analytical methodology

Figure 3.a shows a schematic representation of external pressure distributions on the building envelope at a certain instant, the exerted shear forces, F_X and F_Y, along the two orthogonal axes of the buildings, as well as the torsional moment, M_T, at the geometric centre of the building. Pressure measurements are scanned simultaneously. The instantaneous wind force at each pressure tap is calculated according to:

$$f_{i,t} = p_t \times A_{i,\,\text{effective}} \qquad f_{j,t} = p_t \times A_{j,\,\text{effective}} \tag{1}$$

Where p_t, is instantaneous pressure measured at each pressure tap. $A_{i,\,\text{effective}}$, $A_{j,\,\text{effective}}$ are effective areas for the pressure taps allocated in X-direction and Y-directions, respectively. The wind forces exerted at pressure tap locations in X- and Y-directions are noted by $f_{i,t}$ and $f_{j,t}$, respectively. For each wind direction, the horizontal force components in X- and Y-directions and the total base shear are evaluated according to:

$$F_X = \sum_{i=1}^{N} f_{i,t} \qquad F_Y = \sum_{j=1}^{M} f_{j,t} \qquad V = \sqrt{F_X^2 + F_Y^2} \tag{2}$$

where N and M are the numbers of pressure taps on the longitudinal and transverse directions, respectively. To compare easily the results of this study with design load cases stated in the NBCC wind load provisions, shear coefficients were referred to be in X- and Y-directions or in transverse- and longitudinal-directions, as can be seen in Figure 3.b. This is different from previous studies expressing their results in terms of drag and lift coefficients. In this study, the torsional moment is estimated as follows:

$$M_T = \sum_{i=1}^{N} f_{i,t} * r_i + \sum_{j=1}^{M} f_{j,t} * r_j \qquad (4)$$

where r_i and r_j are the perpendicular distances between the pressure taps and the building center in X- and Y-directions, respectively.

All these forces are normalized with respect to the dynamic wind pressure at the mean roof height as follows:

$$C_{Sx} = \frac{F_X}{q_h B^2} \qquad C_{Sy} = \frac{F_Y}{q_h B^2} \qquad (3)$$

where q_h = dynamic wind pressure (kN/m^2) at mean roof height h (m), B = smallest horizontal building dimension (m). The torsional coefficient, C_T, and equivalent eccentricity, e, are evaluated based on:

$$C_T = \frac{M_T}{q_h B^2 L} \qquad e = \frac{M_T}{V} \tag{4}$$

where L= largest horizontal building dimension

It is recognized that different normalization factors for shear and torsion coefficients have been used in the literature. However, the definitions used herein were selected for better presentation of the effect of building height on the variation of shear and torsional coefficients for all tested buildings.

In addition, for the scope of comparisons with the NBCC wind load provisions, eccentricity and torsional coefficient were also calculated in the transverse direction, as follows:

$$e_y(\%) = e \times \frac{F_X}{V} \times \frac{1}{L} \text{x} 100 \tag{5}$$

$$C_{Tx} = C_{Sx} \times e_y \tag{6}$$

Similarly, the eccentricity and torsion coefficient in longitudinal direction were evaluated based on:

$$e_x(\%) = e \times \frac{F_Y}{V} \times \frac{1}{B} \text{x} 100 \tag{7}$$

$$C_{Ty} = C_{Sy} \times e_x \times \frac{B}{L} \tag{8}$$

All peak shear and torsional coefficients ($|C_{Sx}|_{Max.}, |C_{Sy}|_{Max.}, |C_T|_{Max.}, |C_{Tx}|_{Max.}, |C_{Ty}|_{Max.}$) were considered as the average of the maximum ten values occurring within a 1-hr full-scale equivalent time history of the respective signal. This approach has been considered as a good approximation to the mode value of detailed extreme value distribution and it has been used in previous wind tunnel studies. Recently, in a similar approach used by Keast et al. (2012), the peaks were evaluated as the average of the 10 highest values from 10 one-hour equivalent samples. Although the two approaches are not identical, comparison between the two methods has yielded similar shear and torsion coefficients of buildings tested in similar experimental conditions. The corresponding shear force ($|C_{Sx}|_{corr.}, |C_{Sy}|_{corr.}$) and torsion ($|C_T|_{corr.}, |C_{Tx}|_{corr.}, |C_{Ty}|_{corr.}$) coefficients were evaluated as the average of ten values occurring simultaneously with the ten peaks used to define the respective source maximum value.

5 Experimental results

The two buildings with 0^o and 45^o gabled-roof angles were tested in open terrain exposure at different eave heights (H = 6, 12, 20, 30, 40, 50, and 60 m) for different wind directions (0^o to 90^o every 15^o intervals). Figure 4 presents the variation of the maximum torsion coefficient ($|C_T|_{Max}$) with wind direction for the two buildings tested at different heights. As can be seen from the figure, $|C_T|_{Max}$ has increased significantly when the building height was increased from 6 to 60 m for both buildings with 0^o and 45^o roof angles. The lowest torsional coefficients are found for wind direction around 60^o for all heights. The $|C_T|_{Max}$ occurs for wind directions ranging from 15^o to 45^o for the first three buildings (6, 12, 20 m) while for the other heights, another peak torsional coefficient zone has been recorded for wind directions between 75^o and 90^o. This may

be attributed to different characteristics of wind flow interactions with buildings of heights lower than 20 m, particularly flow reattachment and 3-dimensionality compared to taller buildings.

Figures 5 and 6 show the measured peak shear coefficients in X-direction ($|C_{Sx}|_{Max}$), and Y-direction ($|C_{Sy}|_{Max}$) when the two buildings were tested at different eave heights (H) for different wind directions. As expected, the $|C_{Sx}|_{Max}$ decreases when the wind direction varies from 0^o to 90^o, as shown in Figure 5. On the other hand, for the same wind direction range the $|C_{Sy}|_{Max}$ somewhat increases. The peak values for the $|C_{Sx}|_{Max}$ occur for wind direction ranging from 0^o to 45^o; whereas the peak values for $|C_{Sy}|_{Max}$ occur for wind angles that are almost perpendicular to the building face, (75^o to 90^o). The significant effect of increasing the building height and the roof slope on the generated shear forces is clear. $|C_{Sx}|_{Max}$ has increased by almost 3 and 2 times when the eave height increases from 20 to 60 m for the buildings with flat roof and gabled-roof (45^o), respectively. Changing roof angle from 0^o to 45^o results in increasing $|C_{Sx}|_{Max}$ by about 2.5 times for buildings with a 20 m eave height. This increase in $|C_{Sx}|_{Max}$ is smaller for higher buildings and reaches a 1.5 factor for the 60 m high building. Thus, it is clear that the effect of increasing roof slope on the $|C_{Sx}|_{Max}$ decreases with increasing building height. This may be attributed to the reduction of the ratio of the inclined roof area facing wind relative to the total surface building area as the building height increases from 20 to 60 m. The $|C_{Sx}|_{Max}$ has not been affected much by changing wind incidence from 0^o to 45^o while rapid decrease was noticed from 45^o to 90^o. Similar to the shear force in X-direction, the $|C_{Sy}|_{Max}$ increases about 2.8 times by increasing the height of the flat-roofed building from 20 to 60 m and by about 1.8 times for the gabled-roof (45^o) building. Changing the roof angle from 0^o to 45^o results in doubling $|C_{Sy}|_{Max}$ for the building with eave height of 20 m, yet it resulted in only 30% increase for the 60 m high

building. The maximum shear coefficient in Y-direction has not been affected much by changing wind direction from 45^o to 90^o while rapid decrease occurred from 45^o to 0^o, as expected.

6 Comparison with previous studies

A comparison of the results with those by Keast et al. (2012) for a building with a flat roof and dimensions L = 40 x B = 20 x h = 60 m was made using the wind tunnel measurements in the current study for a building model with L = 61 x B = 39 x h = 60 m. Keast et al. (2012) used shear and torsional coefficients defined as; C_{drag} = Base shear/(q_h Lh) and C_T = Base torsion/ (q_h L^2h), respectively (where q_h = dynamic wind pressure at mean roof height, L = largest horizontal building dimension, H = h = mean roof height = eave height - flat roof). For comparison purposes, the results of the current study have been transformed to these same definitions. Additionally, shear coefficients for only 0^o and 90^o wind directions were considered in this comparison, as Keast et al. (2012) introduced shear force in terms of drag and lift force coefficients. Table 2 presents the experimental parameters, as well as the evaluated shear and torsional coefficients for the buildings examined. Figure 7 shows the mean and peak (maximum and minimum) torsional coefficients for different wind directions evaluated by the two studies. Results show relatively good agreement for the measured shear forces and torsion in these studies. Small differences could be attributed to the difference in building dimensions and the terrain exposure.

Another comparison with the study by Tamura et al., (2003) for a building with dimensions L = 50 x B = 25 x h = 50 m was made using the building model representative of L = 61 x B = 39 x h = 50 m. The two flat-roofed buildings have the same height and similar aspect ratios of their plan

dimensions L/B = 2 and 1.56. In this comparison, the definitions of torsional and shear coefficients in the Tamura et al. (2003) study were followed. The torsional coefficient was defined as C_T = Base torsion/(q_h LhR) where; R=$\sqrt{(L^2+B^2)}/2$, B = smallest horizontal building dimension, and shear coefficient C_{drag}= Base shear/(q_h Lh). For this comparison, only wind direction perpendicular to the largest horizontal building dimension was considered due to the lack of data for other cases in Tamura et al. (2003). Table 3 shows the building/exposure parameters together with the results. Higher coefficients are shown in Tamura et al. (2003); this may be due to the geometric and terrain exposure differences used in the two studies. Indeed, the mean wind velocity at the mean roof building height in urban terrain is much lower than that in open terrain exposure.

In AIJ-RLB (2004), torsion for low- and medium-rise buildings is implicitly considered on the applied drag and lift uniform forces (i.e. X- and Y-shear force components). The AIJ-RLB (2004) provisions were developed mainly by evaluating wind load effects on one structural building system (i.e. building with only four corner columns), as presented by Tamura et al. (2003, 2008). Hence, the effect of applying the measured wind forces components on the calculated normal stress on these four corner columns was used to determine the load combinations presented in the AIJ-RLB (2004). Additional comparison between the AIJ-RLB (2004) and the current study is conducted for a flat-roofed building -similar to one tested in the current study- with the full scale dimensions (L = 61 x B = 39 x h = 60 m). Two main structural systems were considered for this comparison. The first system consisted of shear walls at the exterior building perimeter and the other with shear walls near the building core (see Figure 8). In the AIJ-RLB calculations, the gust factor was taken as 2. It was found that for a building with

structural system 1, AIJ-RLB (2004) gives 10% higher resultant design force for designing the shear wall as compared to the current study, whereas for system 2, AIJ-RLB (2004) underestimates the resultant design force by about 30%.

7 Comparison with NBCC (2010)

The experimental results were used to introduce four load cases, namely: shear and torsion load cases in both transverse and longitudinal wind directions (see Table 4). These load case values were compared to the evaluated shear and torsion values by the NBCC (2010). In the shear load case, maximum shear was considered along with the corresponding torsion, whereas in the torsion load case, maximum torsion and the corresponding shear were evaluated. The most critical shear and torsion values reported for wind direction range of 0^o to 45^o were considered in the transverse load cases; and from 45^o to 90^o in the longitudinal load cases. Furthermore, in transverse torsion load case, maximum torsion ($|C_{Tx}|_{Max.}$) resulting from winds in only transverse direction ($|C_{sx}|_{corr.}$) was considered. Similarly, $|C_{Ty}|_{Max.}$ and $|C_{sy}|_{corr.}$ were evaluated for comparison in the longitudinal torsion load case. Transverse shear load case was also defined as the maximum shear force ($|C_{sx}|_{Max.}$) and the corresponding torsion ($|C_{Tx}|_{corr.}$) while in the longitudinal shear load case ($|C_{sy}|_{Max.}$) and ($|C_{Ty}|_{corr.}$) were considered. The eccentricities were noted by e_x and e_y in transverse- and longitudinal-direction as defined in Eqs. 5 and 7 and shown in Figure 3.b.

In NBCC (2010), the static method is introduced for low-rise buildings while the simplified method is proposed for medium-rise buildings. The static method calculations for the torsional and shear coefficients were derived based on figure I-7 in Commentary I of NBCC 2010, where the external peak (gust) pressure coefficients (C_pC_g) are provided for low-rise buildings.

Likewise, for the simplified method, the external pressure is taken from figure I-15, Commentary I. Partial and full load cases were considered to estimate maximum torsion and corresponding shear, as well as maximum shear and corresponding torsion. Calculations were carried out considering the open terrain exposure. Static method values were increased by 25% to eliminate the implicit reduction (0.8) due to several factors including directionality (Stathopoulos, 2003).

Figure 9 shows the wind tunnel results along with the torsional load case parameters evaluated by the static and simplified methods in the transverse direction. Although the static method requires applying higher loads in comparison with wind tunnel measurements, it significantly underestimates torsion on low-rise buildings. This is mainly due to the fact that it specifies a significantly lower equivalent eccentricity (e_y (%)) which is about 3% of the facing horizontal building dimension compared to the equivalent eccentricity evaluated in the wind tunnel tests which is around 8% and 15% for buildings with gabled and flat roof, respectively. Also, for the building with a flat roof, the simplified method requires applying almost the same wind loads as those measured in the wind tunnel. The eccentricity specified by the simplified method is 25% of the facing building width, which is significantly higher than the measured eccentricity (i.e. about 15%), hence the evaluated torsion using the simplified method exceeds the measured torsion significantly. For the building with 45^o roof, the corresponding shear seems to exceed that on the flat-roofed building by 50%. However lower eccentricities were noticed for buildings with roof angle 45^o.

Figure 10 presents the shear load case in the transverse direction evaluated by NBCC (2010) and measured in the wind tunnel. The static method compares well with the wind tunnel measurements in evaluating maximum shear while it underestimates the corresponding torsion on low-rise building with 45^o. The simplified method overestimates shear on buildings with flat

roofs, however it underestimates shear on building with 45^{o} roof angle with heights up to 40 m. Moreover, the simplified method neglects the corresponding torsion by applying wind loads uniformly distributed to evaluate maximum shear; this may be inadequate for the design of buildings sensitive to torsion.

Similarly, Figures 11 and 12 present torsional and shear load cases in the longitudinal direction. In this direction, the NBCC static method also significantly underestimates the maximum torsion on low-rise buildings with flat roofs. As Figure 11 shows, the measured eccentricity in the wind tunnel for low-rise buildings is about 25% of building width (B). The static method applies higher than the measured corresponding shear force with eccentricity of 5%. For buildings with flat roofs, the simplified method compares well with wind tunnel in predicting the maximum torsion and overestimates maximum shear; while, the simplified method underestimates maximum torsion and succeeds in predicting maximum shear on buildings with 45^{o} roof angle. However, the corresponding shear estimated by the simplified method shows good agreement with the wind tunnel data but the equivalent eccentricity for the building with gabled-roof is low. Figure 12, also shows that the corresponding torsion to the maximum shear has been neglected completely in longitudinal direction, as in Figure 10 for transverse direction. Neglecting the corresponding torsion, as mentioned previously, may not be always prudent.

8 Suggested load cases to account for torsion on rectangular buildings

Table 5 summarizes the shear force coefficients ($|C_{sx}|_{Max.}$, $|C_{sy}|_{Max.}$) evaluated by the wind tunnel measurements for the two buildings (i.e. with flat and gabled roof) tested at all different heights

in open terrain exposure. Based on the wind tunnel results, Table 6 presents the suggested wind load cases for the design of low- and medium-rise buildings with rectangular plan and different roof slopes. Shear and torsion load cases are provided for transverse and longitudinal directions. The shear load cases were defined by applying the maximum shear force in X-direction at an eccentricity e_y(%) from facing horizontal building dimension. For buildings with flat and gabled roof, the corresponding torsion is presented for the suggested shear load cases by applying the maximum wind load at eccentricity of 5%, 15% from the facing horizontal building dimension in transverse- and longitudinal-direction, respectively. Torsion load case is defined by applying 80% of the maximum shear force but at higher eccentricities as shown in Table 6. Although the current study tested only buildings with aspect ratio (L/B) of 1.6, the authors believe that the proposed load cases could be applied for buildings with aspect ratios from 1.6 to 2. This is based on the comparisons with limited previous studies. For instance, Keast et al (2012) showed that for a 60 m high flat roof building with aspect ratio (L/B) equal to 2, the maximum torsion was associated with 80% of the maximum shear force for wind directions 0^o and 90^o. Also, the associated eccentricities were about 8%, 43% from the facing horizontal building dimension for 0^o and 90^o wind directions, respectively. It should be noted that the 43% eccentricity in the longitudinal direction is higher than the 35% proposed value obtained from considering only the torsion due to winds in longitudinal direction. The difference may be attributed to the contribution to the total torsion of the corresponding shear force component in the transverse direction. Clearly, more experimental work for buildings with different aspect ratios would be significant to confirm and generalize the current findings.

It was also quite interesting to see the difference between the current analytical approaches stated in NBCC (2010) to evaluate torsion on buildings and the suggested load cases. Figure 13 shows

this comparison in transverse direction for buildings with flat and gabled roof. The suggested approach introduces lower torsion in the transverse direction (see Figure 13), but higher torsion in the longitudinal direction as this is underestimated using NBCC (2010) - see Figure 11.

9 Summary and conclusions

Wind-induced torsion and shear were measured in the wind tunnel for buildings having the same horizontal dimensions, different roof angles (0^o and 45^o) and heights ranging from 6 m to 60 m. In addition, the experimental results were compared with the wind load provisions of NBCC (2010). The analysis of experimental results and comparisons with codes/standards demonstrate the following:

For low-rise buildings, the static method in the NBCC (2010):

- underestimates torsion significantly;
- compares well with the maximum shear evaluated in the wind tunnel; and
- succeeds to predict corresponding torsion for buildings with flat roofs but not always for buildings with 45^o roof angle

For medium-rise buildings, the simplified method in the NBCC (2010):

a- In the Transverse direction:

- overestimates maximum torsion and shear on buildings with flat roofs.
- overestimates maximum torsion and underestimates maximum shear on buildings with roof angle 45^o and heights up to 40 m.

b- In the Longitudinal direction:

- compares well with wind tunnel measurement results in evaluating maximum torsion, while it overestimates maximum shear on buildings with flat roofs.
- underestimates maximum torsion but succeeds to evaluate maximum shear on buildings with roof angle of 45º.

Finally, shear and torsion load cases were suggested for better evaluation of wind loads including torsion for the design of rectangular buildings with horizontal aspect ratios L/B = 1.6 to 2.

10 Acknowledgment

The authors are grateful for the financial support received for this study from the Natural Sciences and Engineering Research Council of Canada (NSERC), as well as le Fonds de Recherche du Québec - Nature et Technologies (FRQNT) and le Centre d'Études Interuniversitaire sur les Structures sous Charges Extrêmes (CEISCE).

11 References

AIJ-RLB, 2004. Recommendations for loads on buildings. Architectural Institution of Japan, Tokyo.

ASCE, 1999. Wind tunnel studies of buildings and structures. ASCE Manuals and Reports on Engineering Practice No. 67, ASCE, Reston, Virginia, 207 pp.

Boggs, D. W., Hosoya, N. and Cochran, L. 2000. Source of torsional wind loading on tall buildings-lessons from the wind tunnel. *In* Proceedings of the Structures Congress, Sponsored by ASCE/SEI, Philadelphia, May.

Elsharawy, M., Stathopoulos, T., and Galal, K. 2012. Wind-Induced torsional loads on low buildings. Journal of Wind Engineering and Industrial Aerodynamics, 104-106: 40-48.

Isyumov, N. 1982. The aeroelastic modelling of tall buildings. International workshop on wind tunnel modeling criteria and techniques in civil engineering applications. Gaithersburg, Maryland, April 1982. Cambridge University Press: 373-407.

Isyumov, N., and Case, P. C. 2000. Wind-Induced torsional loads and responses of buildings. In Proceedings of the Structures Congress, Sponsored by ASCE/SEI, Philadelphia, May.

Keast, D.C., Barbagallo, A., and Wood, G.S. 2012. Correlation of wind load combinations including torsion on medium-rise buildings. Wind and Structures, An International Journal, 15(5): 423-439.

Melbourne, W.H. 1975. Probability distributions of response of BHP house to wind action and model comparisons. Journal of Wind Engineering and Industrial Aerodynamics, 1(2): 167-175.

NBCC 2010. User's Guide – NBC 2010, Structural Commentaries (part 4). Issued by the Canadian Commission on Buildings and Fire Codes, National Research Council of Canada.

Sanni, R. A., Surry, D., and Davenport, A. G. 1992. Wind loading on intermediate height buildings. Canadian Journal of Civil Engineering, 19: 148-163.

Stathopoulos, T. 2003. Wind Loads on Low Buildings: In the Wake of Alan Davenport's Contributions. Journal of Wind Engineering and Industrial Aerodynamics, 91(12-15): 1565-1585.

Stathopoulos, T., and Dumitrescu-Brulotte, M. 1989. Design recommendations for wind loading on buildings of intermediate height. Canadian Journal of Civil Engineering, 16: 910-916.

Tamura, Y., Kikuchi, H., Hibi, K. 2001. Extreme wind pressure distributions on low- and middle-rise building models. Journal of Wind Engineering and Industrial Aerodynamics, 89(14-15): 1635-1646.

Tamura, Y., Kikuchi, H., Hibi, K. 2003. Quasi-static wind load combinations for low- and middle-rise buildings. Journal of Wind Engineering and Industrial Aerodynamics, (91): 1613-1625.

Van der Hoven, I. 1957. Power spectrum of wind velocities fluctuations in the frequency range from 0.0007 to 900 Cycles per hour." Journal of Meteorology, (14): 160-164.

Vickery, B.J., Basu, R.I. 1984. The response of reinforced concrete chimneys to vortex shedding. Engineering Structures, (6): 324-333.

List of Symbols

q_h = dynamic wind pressure

$|C_{Sx}|_{corr.}$ = corresponding shear force coefficient in transverse direction

$|C_{Sx}|_{Max.}$ = peak shear force coefficient in transverse direction

$|C_{Sy}|_{corr.}$ = corresponding shear force coefficient in longitudinal direction

$|C_{Sy}|_{Max.}$ = peak shear force coefficient in longitudinal direction

$|C_T|_{Max.}$ = Peak torsional coefficient

$|C_{Tx}|_{Max.}$ = peak torsional coefficient due to winds in transverse direction

$|C_{Ty}|_{Max.}$ = peak torsional coefficient due to winds in longitudinal direction

B = smallest horizontal building dimension

C_{Sx} = shear coefficient in X-direction

C_{Sy} = shear coefficient in Y-direction

$C_{T\,Mean}$ = mean torsion coefficient

C_{Tx} = torsional coefficient due to winds in transverse direction

C_{Ty} = torsional coefficient due to winds in longitudinal direction

e, e_x, e_y = eccentricities

$f_{i,t}$, $f_{j,t}$ = wind forces at pressure taps

f_n = building natural frequency

F_X, F_Y = horizontal force components

h = mean roof height

H = eave building height

L = largest horizontal building dimension

M_T = torsional moment

p_t = instantaneous pressure at pressure taps

$A_{i,\,effective}$ = area effective for pressure tap allocated in X-direction

$A_{j,\,effective}$ = area effective for pressure tap allocated in Y-direction

r_i , r_j = perpendicular distances between the pressure taps and the building center in X- and Y-directions, respectively

V = total base shear force

Z = height from the ground

Z_g = gradient height

α = power law index

List of Figures:

Fig. 1: Wind tunnel models: A) Building with a flat roof (0^o), B) Building with a gabled-roof (45^o)

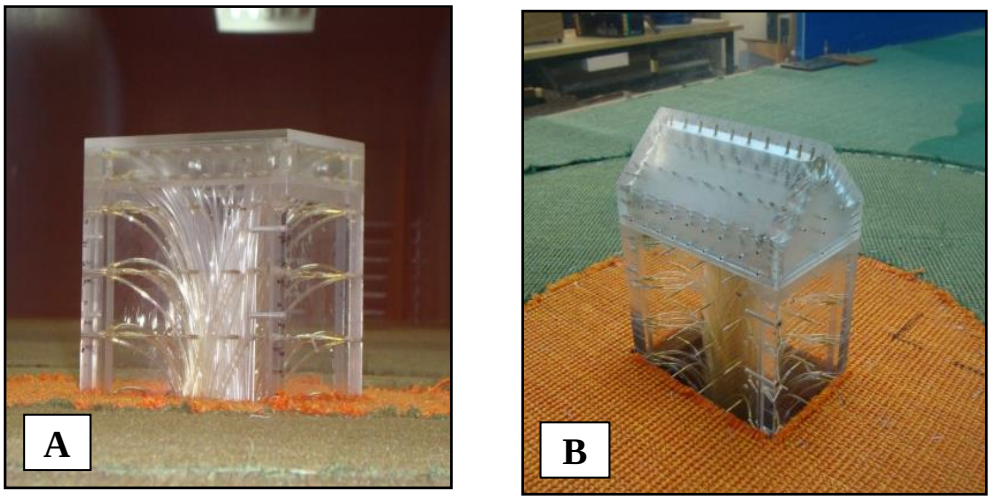

Fig. 2: Wind velocity and turbulence intensity profiles for open terrain exposure

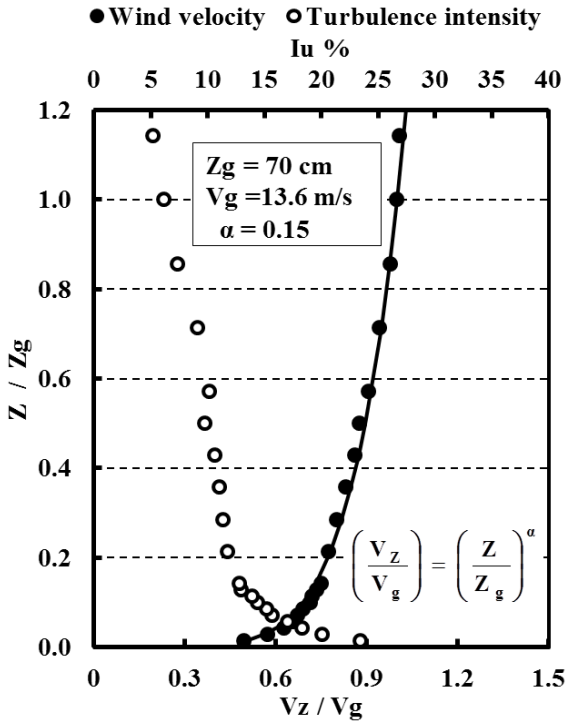

Fig. 3.a: Measurement procedure for horizontal wind forces, F_X and F_Y, and torsional moment, M_T

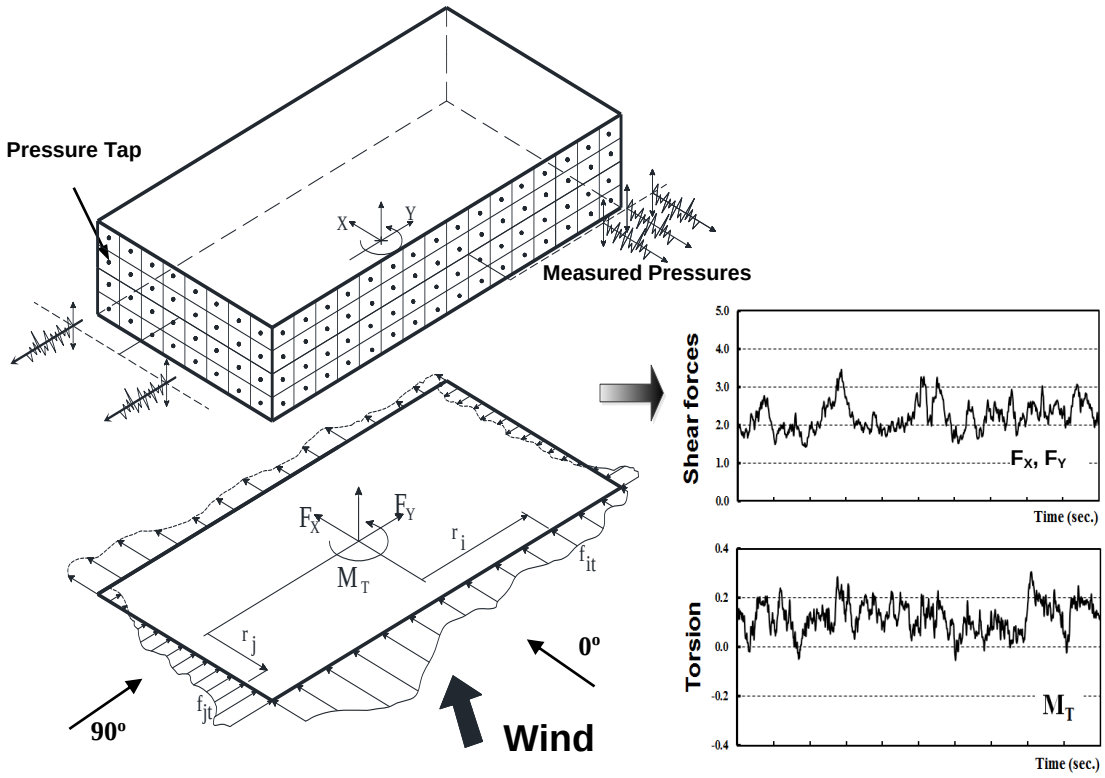

Fig. 3.b: Resultant and wind force components along with the eccentricities in transverse (X) and longitudinal (Y) directions

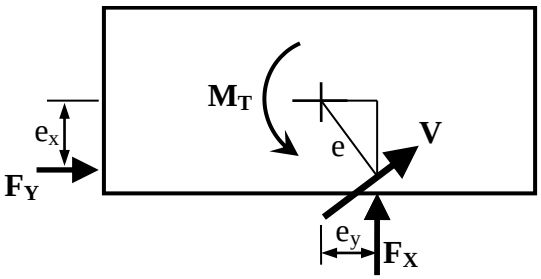

Fig. 4: Variation of peak torsion coefficient ($|C_T|_{Max.}$) with wind direction for the tested buildings with flat and gabled roof

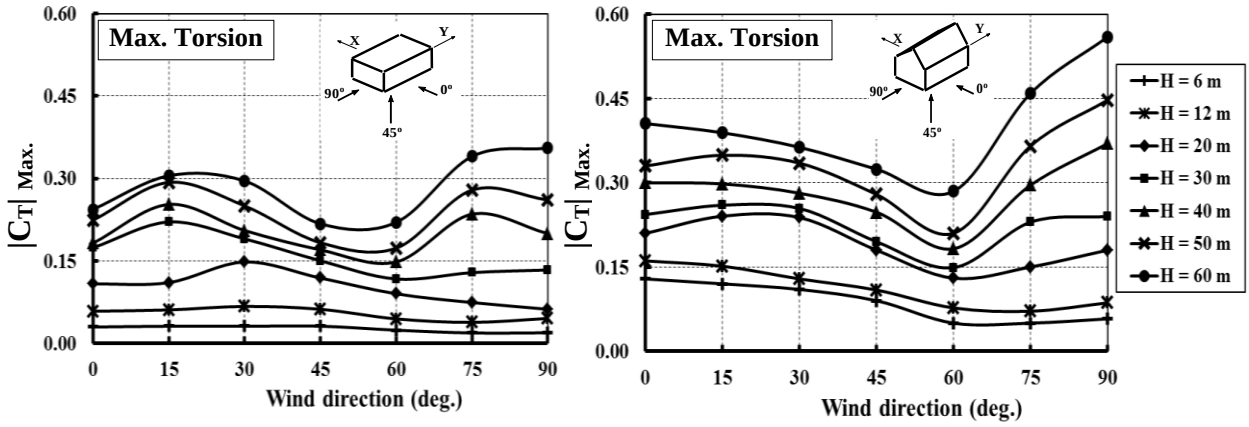

Fig. 5: Variation of peak shear coefficient ($|C_{Sx}|_{Max.}$) with wind direction for the tested buildings with flat and gabled roof

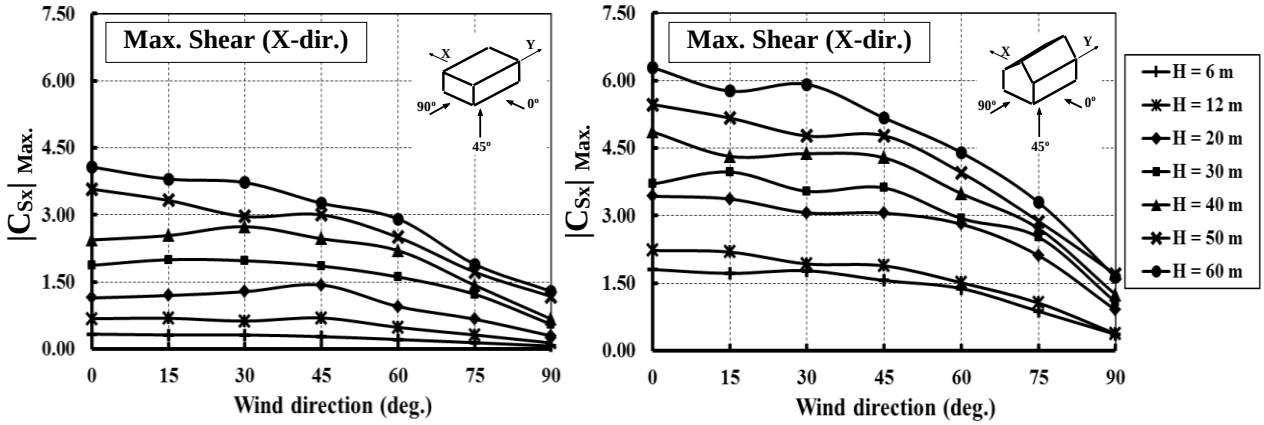

Fig. 6: Variation of peak shear coefficient ($|C_{Sy}|_{Max.}$) with wind direction for the tested buildings with flat and gabled roof

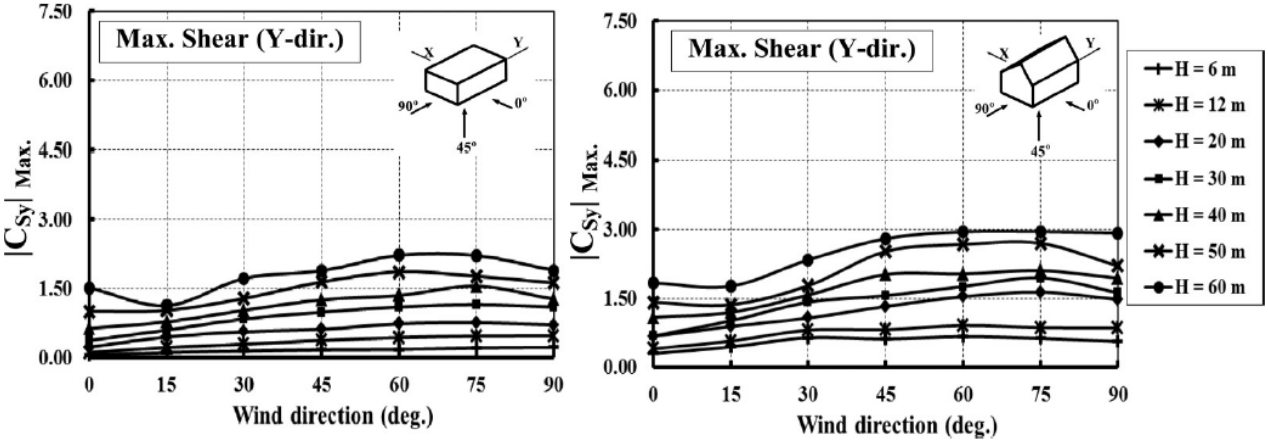

Fig. 7: Comparison of peak and mean torsional coefficients with those from Keast et al. (2012) for two flat roof buildings with 60 m height

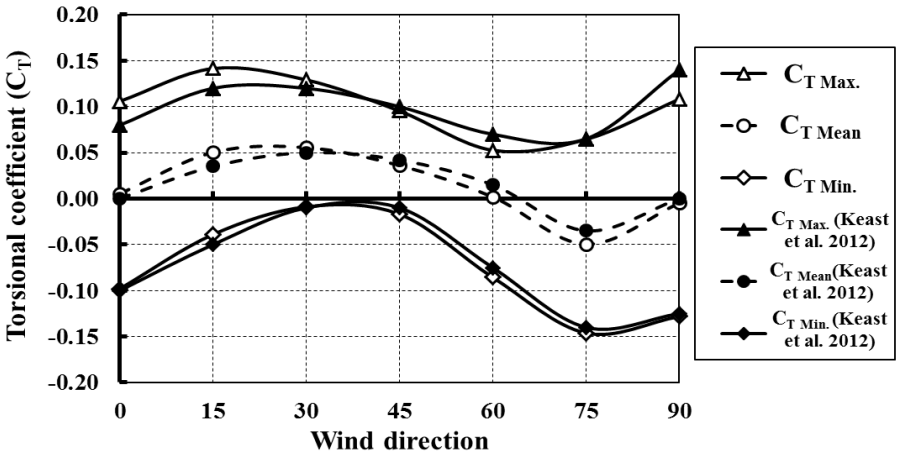

Fig. 8: Sketch for the two structural systems considered for the comparison with AIJ-RLB (2004)

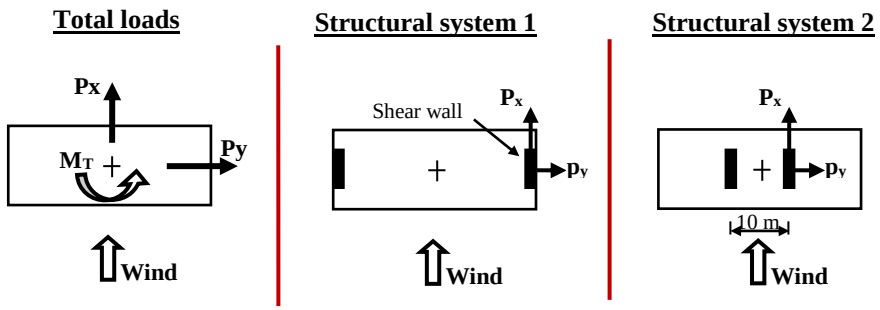

Fig. 9: Comparison of torsional load case evaluated using NBCC (2010) and wind tunnel measurements for buildings with 0º and 45º roof angles (Transverse direction)

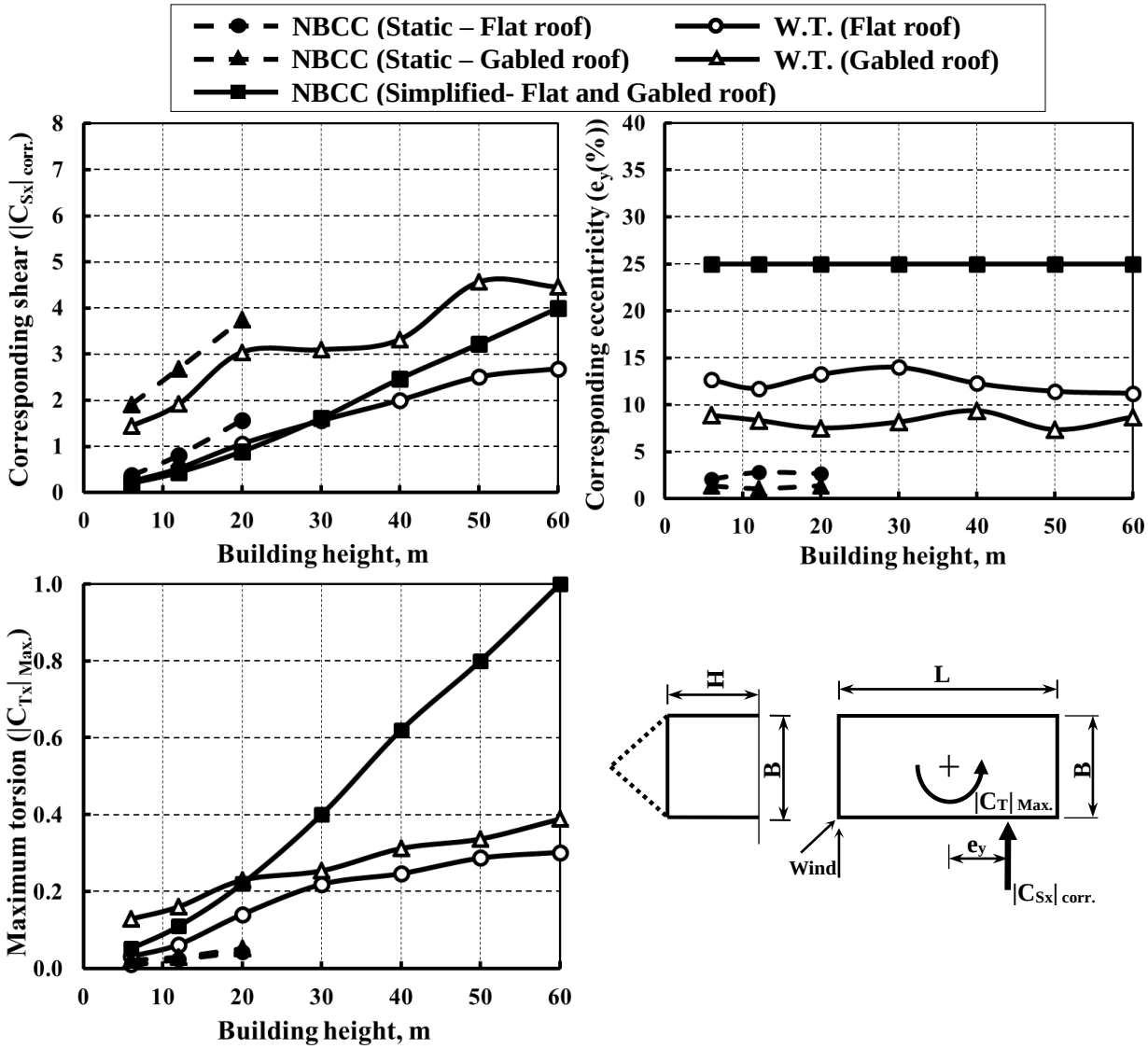

Fig. 10: Comparison of shear load case evaluated using NBCC (2010) and wind tunnel measurements for buildings with 0º and 45º roof angles (Transverse direction)

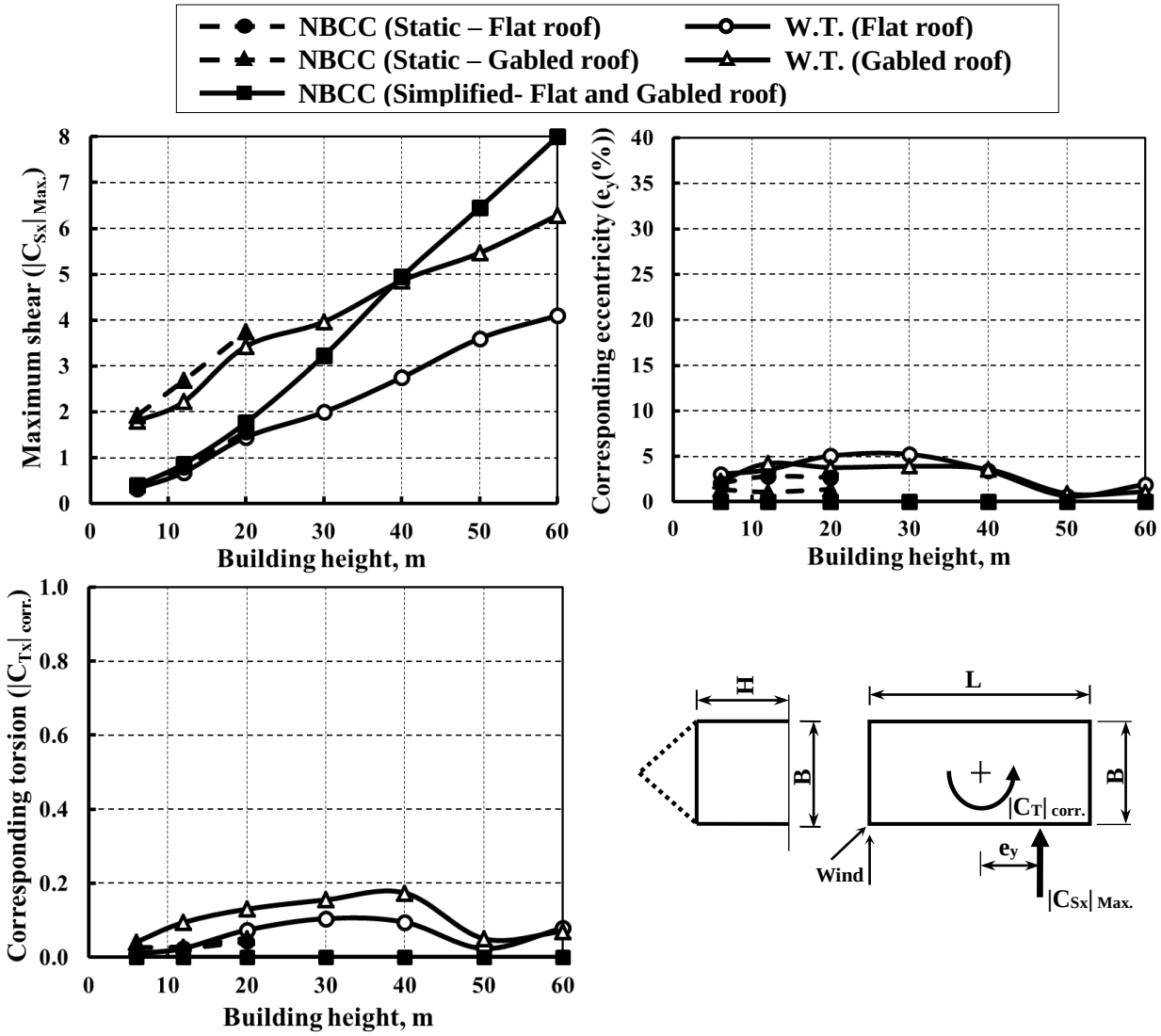

Fig. 11: Comparison of torsional load case evaluated using NBCC (2010) and wind tunnel measurements for buildings with 0^o and 45^o roof angles (Longitudinal direction)

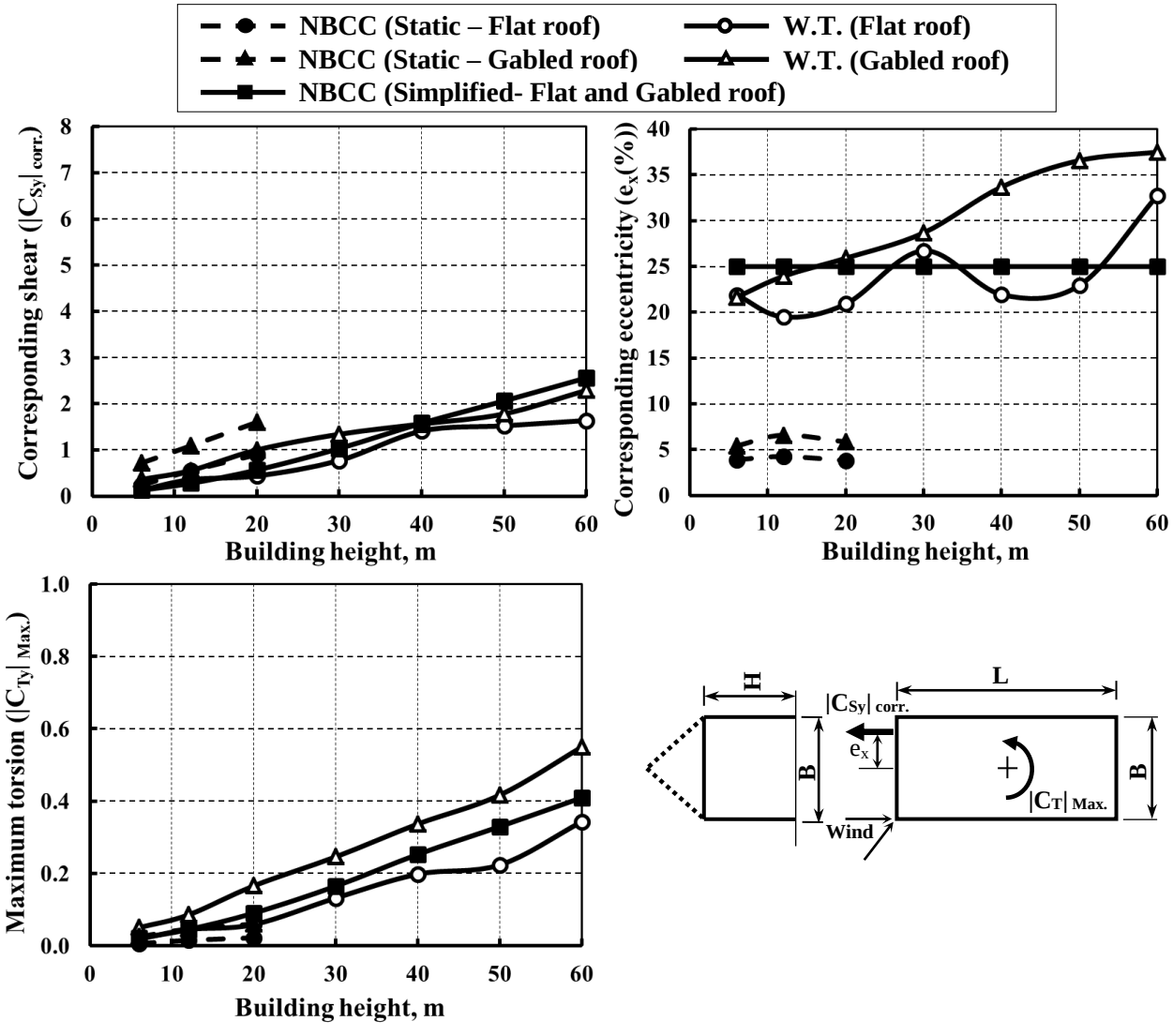

Fig. 12: Comparison of shear load case evaluated using NBCC (2010) and wind tunnel measurements for buildings with 0º and 45º roof angles (Longitudinal direction)

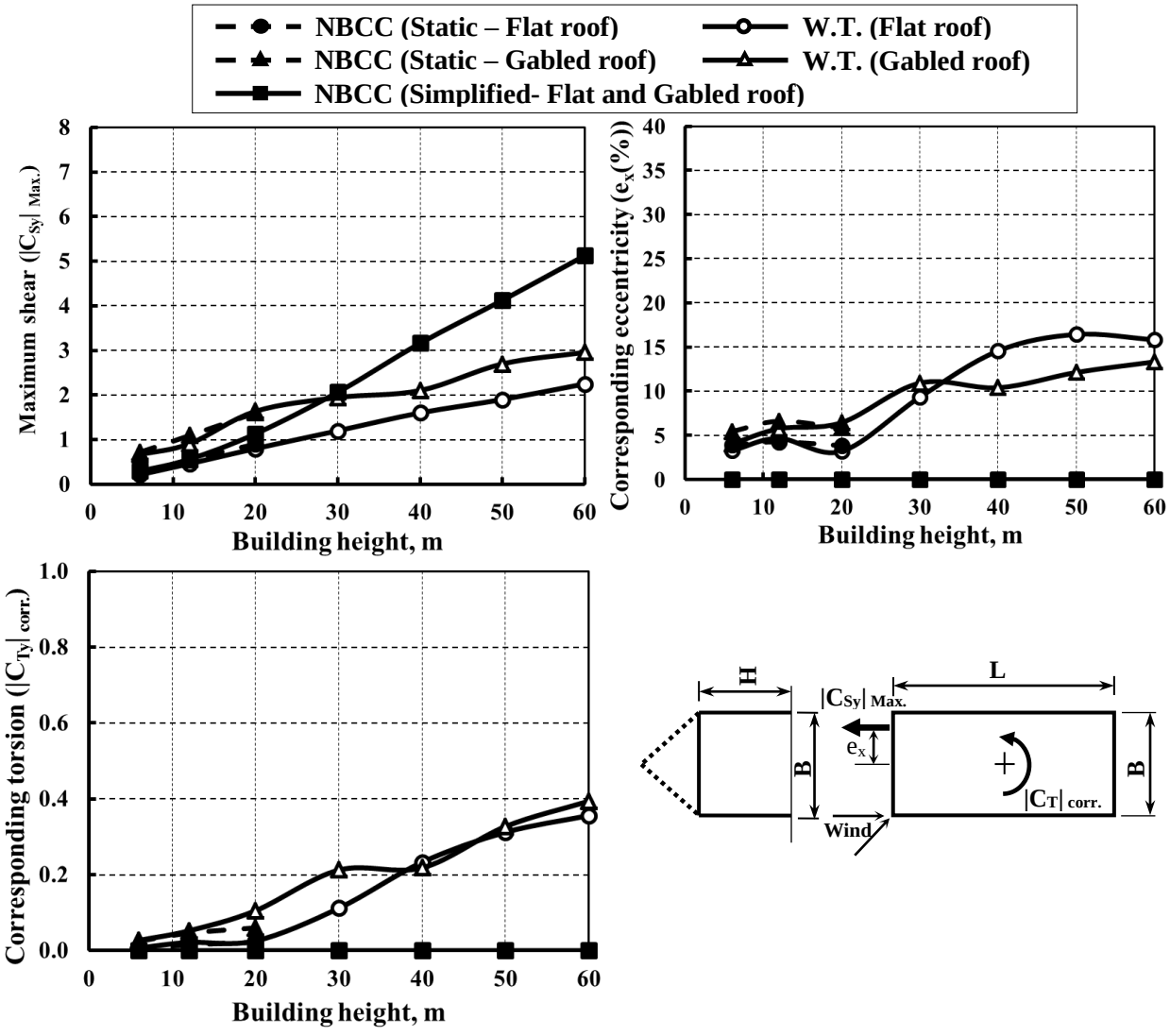

Fig. 13: Maximum torsion evaluated using NBCC (2010), wind tunnel measurements and suggested approach in transverse direction for buildings with: a) flat roof; b) gabled roof

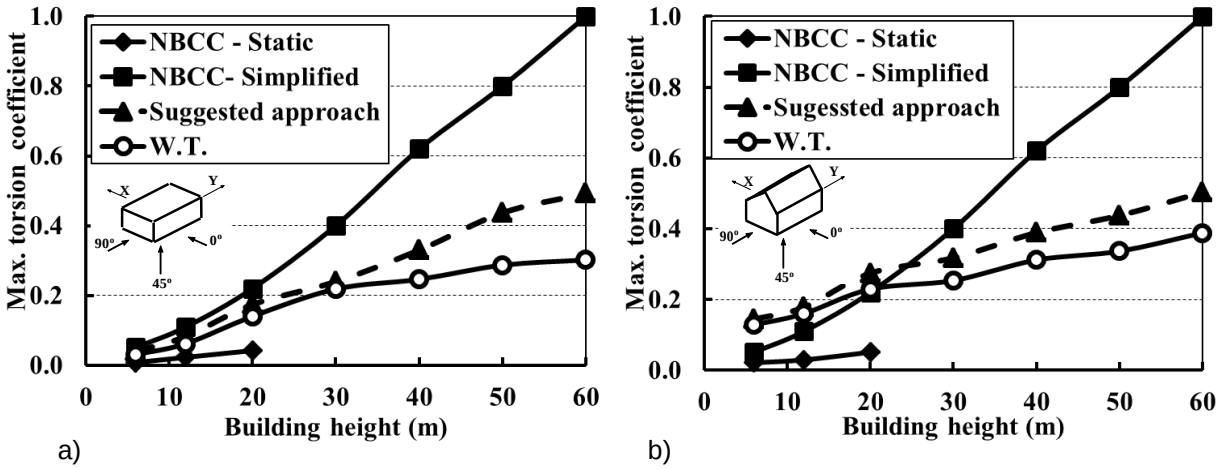

List of tables:

Table 1. Model dimensions and building heights tested in the boundary layer wind tunnel

Building	Dimensions	
	Scaled (1:400, mm)	Actual (m)
Width (B)	97.5	39
Length (L)	152.5	61
Tested heights (H)	15, 30, 50, 75, 100, 125, 150	6, 12, 20, 30, 40, 50, 60

Table 2: Comparison of peak torsion and shear coefficients with Keast et al. (2012)

	Keast et al. 2012	Current study
Wind tunnel technique	6 degree-of-freedom high frequency balance	High frequency pressure integration
Building dimensions (m)	L = 40 x B = 20 x h = 60	L = 61 x B = 39 x h = 60
Roof	Flat	Flat
Aspect ratio (L/B)	2	1.56
Scale	1:400	1:400
Model dimensions (mm)	100 x 50 x150	152.5 x97.5 x150
Terrain exposures	Open	Open
Wind direction	0^o to 90^o @ 15^o	0^o to 90^o @ 15^o
Torsion coefficient ($\|C_T\|_{Max.}$)	0.14	0.15
Shear coefficient ($\|C_{Sx}\|_{Max.}$, 0^o)	(C_{drag}, 0^o) = 2.00	1.70
Shear coefficient ($\|C_{Sy}\|_{Max.}$, 90^o)	(C_{drag}, 90^o) = 0.75	0.80

Table 3. Comparison of peak torsion and shear coefficients with Tamura et al. (2003)

Experimental variables	Tamura et al. 2003	Current study
Wind tunnel technique	High frequency pressure integration	High frequency pressure integration
Building dimensions (m)	L = 50 x B = 25 x h = 50	L = 61 x B = 39 x h = 50
Aspect ratio (L/B)	2.0	1.56
Roof	Flat	Flat
Scale	1:250	1:400
Model dimensions (mm)	100 x 100 x 200	152.5 x 97.5 x 125
Terrain exposures	Urban (α= 0.25)	Open (α= 0.15)
Wind direction	$\perp$ to building length (L= 50 m)	$\perp$ to building length (L= 61 m)
Torsion coefficient ($\lvert C_T \rvert_{Max.}$)	0.30	0.20
Shear coefficient ($\lvert C_{Sx} \rvert_{Max.}$)	3.00	1.90
Shear coefficient ($\lvert C_{Sy} \rvert_{Max.}$)	0.90	0.50

Table 4. Wind load cases in transverse and longitudinal directions

Load case	Transverse direction	Longitudinal direction
Shear	Max. shear in X-dir. ($\|C_{sx}\|_{Max.}$) and corresponding torsion ($\|C_{Tx}\|_{Corr.}$)	Max. shear in Y-dir. ($\|C_{sy}\|_{Max.}$) and corresponding torsion ($\|C_{Ty}\|_{Corr.}$)
Torsion	Max. torsion ($\|C_{Tx}\|_{Max.}$) and corresponding shear in X-dir. ($\|Cs_{x}\|_{Corr.}$)	Max. torsion ($\|C_{Ty}\|_{Max.}$) and corresponding shear in Y-dir. ($\|Cs_{y}\|_{Corr.}$)

Table 5. Most critical shear coefficients for flat and gabled roof buildings

	Flat Buildings		Gabled roof buildings	
Height (m)	$\|C_{Sx}\|_{Max.}$	$\|C_{Sy}\|_{Max.}$	$\|C_{Sx}\|_{Max.}$	$\|C_{Sy}\|_{Max.}$
6	0.33	0.22	1.80	0.67
12	0.69	0.46	2.22	0.91
20	1.45	0.80	3.43	1.63
30	2.00	1.20	3.97	1.94
40	2.75	1.60	4.86	2.10
50	3.60	1.90	5.47	2.70
60	4.10	2.25	6.29	2.96

Table 6. Suggested load cases for the design of flat or gabled roof rectangular buildings

		Shear load case		Torsion load case	
		wind load	eccentricity	wind load	eccentricity
Flat-roof buildings	Transverse	P_X*	0.05 L	0.8 P_X	0.15 L
	Longitudinal	P_Y**	0.15 B	0.8 P_Y	0.35 B
Gable-roof buildings	Transverse	P_X*	0.05 L	0.8 P_X	0.10 L
	Longitudinal	P_Y**	0.15 B	0.8 P_Y	0.30 B

$P_X^* = |C_{Sx}|_{Max.} * q_h * B^2$ $P_Y^{**} = |C_{Sy}|_{Max.} * q_h * B^2$

Where values for $|C_{Sx}|_{Max}$ and $|C_{Sy}|_{Max}$ would be obtained from Table 5 for different building heights